8–8 Numerical Analysis of Hydrogen Combustion Behavior

—Effects of Temperature and Pressure on Flame Instability—

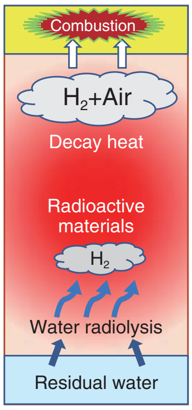

Fig.1 Conceptual diagram of the interior of a storage container for radioactive materials

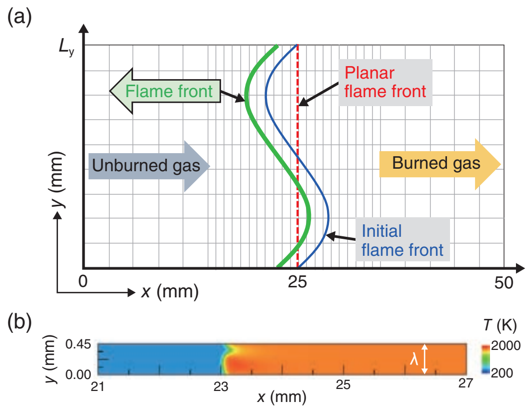

Fig.2 (a) Computational domain and initial flame front position for two-dimensional simulations and (b) temperature distribution of the flame front at 0.5 MPa, 473 K, and 5 ms ($L_y = \lambda$, where L_y is the *y*-axis coordinate and λ is the wavelength of the initial flame front)
Unburned gas flows in from the left, and the burned gas flows out from the right of the computational domain.

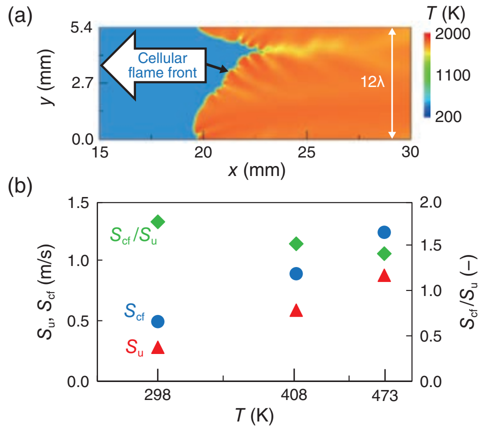

Fig.3 (a) Temperature distribution of cellular flames at 0.5 MPa, 473 K, and 5 ms ($L_y = 12\lambda$) and (b) burning velocities of a planar flame (S_u), cellular flame (S_{cf}), and their relative velocity (S_{cf}/S_u) at 0.5 MPa
Emerging and splitting of the cellular structure on the flame surface are seen clearly in the large-scale domain.

In the decommissioning and waste management of TEPCO's Fukushima Daiichi Nuclear Power Station (FDNPS), hydrogen (H_2) management is an important issue. As shown in Fig.1, residual water in the storage container is decomposed by radiations emitted from the materials to generate H_2. When the H_2 concentration reaches the flammable point, H_2 combustion may occur, and the combustion may be explosive in severe cases, leading to damage to the surrounding facilities and leakage of radioactive materials to the environment. The temperature and pressure may increase because of the decay heat of radioactive materials, and thereby also increasing the risk of H_2 combustion. Thus, understanding the flame of H_2 is necessary for H_2 safety management.

As a part of addressing this issue, we performed simulations on lean H_2-air premixed combustion in two-dimensional flow fields and clarified the detailed structure and propagation process of H_2 flames under high-temperature and high-pressure conditions.

As shown in Fig.2(a), the flame front (green line) comprises a "stable" planar (red line) and an "unstable" sinusoidal initial (blue line) part that propagates toward the unburned flammable gas in the simulation. Fig.2(b) shows the temperature distribution of the flame front. When the *y*-axis coordinate (L_y) corresponds to the wavelength (λ) of the initial flame front, the flame front (border between blue and orange) cannot be seen in detail. When the *y* coordinate is increased, as seen in Fig.3(a) ($L_y = 12\lambda$), the flame front clearly forms an unstable cellular structure.

In this work, the instabilities of the H_2 flames were analyzed by considering the relations between temperature (T) and burning velocities at different pressures (P). When P increased at 298 K, the burning velocity of the planar flame decreased. On the other hand, as shown in Fig.3(b), when T increased at high P, the burning velocity of the planar flame (▲) and that of the cellular flame (●) increased, but the relative velocity (◆) decreased. In addition, the cellular structure of the flame surface became less noticeable. This result indicates that the instability of H_2-air premixed flame decreased when the unburned gas hotter; the combustion became smoother at higher temperatures. Thus, we can conclude that temperature and pressure affect the instability of the flame and the characteristics and behavior of the instability.

Further studies applying three-dimensional flow-field simulations are necessary to clarify the fundamental characteristics of H_2-air combustion and explosion, so that we can provide the necessary knowledge for H_2 safety measures in the decommissioning and high-radioactive waste management of FDNPS.

(Thwe Thwe Aung)

Reference

Thwe Thwe Aung et al., The Effects of Unburned-Gas Temperature and Pressure on the Unstable Behavior of Cellular-Flame Fronts Generated by Intrinsic Instability in Hydrogen-Air Lean Premixed Flames Under Adiabatic and Non-Adiabatic Conditions: Numerical Simulation Based on the Detailed Chemical Reaction Model, Journal of Nuclear Science and Technology, vol.60, issue 6, 2023, p.731–742.